

Multi-body seakeeping design optimization

T.J. Peltzer, B.J. Rosenthal & W.K. Reppun

Navatek, Ltd., Honolulu, Hawaii, USA

D.C. Kring

Flight Safety Technologies, Inc., Mystic, Connecticut, USA

W.M. Milewski & B. Connell

Applied Physical Sciences Corp., Groton, Connecticut, USA

ABSTRACT: Seakeeping performance of multiple bodies operating in close proximity is of interest due to the current US Navy focus on sea basing. This paper describes the application of an enhanced 3D seakeeping code, AEGIR, to a multi-body seakeeping design optimization of a novel offshore platform concept using Particle Swarm Optimization. A framework for this optimization was developed, and an automated control process for that framework was implemented using a Java-based shell; this framework was then successfully applied to a simplified multi-body seakeeping optimization study that explored the effects of different objective functions based on the root mean square motions of the platform. The results show that varying the objective function produces a series of good seakeeping designs from which to choose, depending on the designer's goals.

1 INTRODUCTION

Multi-body seakeeping performance is a problem relevant to many at-sea transfer applications, especially for the US Navy's sea basing initiative to provide offshore staging areas in regions where land-based logistic operations are infeasible. These seabases, consisting of two or more moored vessels, will be located approximately 100 nautical miles offshore where they may be subjected to sea conditions that could potentially limit some operations, such as the transfer of men and matériel between vessels or the launch and recovery of smaller vessels. The development and validation of computer simulation and design tools to predict and minimize multi-body motions in waves will facilitate realization of an effective sea basing capability.

This paper describes the application of a three-dimensional seakeeping code, AEGIR, enhanced to improve its ability to predict the motions of multiple bodies operating in close proximity in waves, to seakeeping design optimization. A novel offshore platform concept, the Articulated Stable Ocean Platform (ASOP), was used as the basis for a simplified multi-body model optimization problem with the goal of reducing seakeeping motions. A seakeeping optimization framework was developed using AEGIR for seakeeping simulations and Particle Swarm Optimization (PSO); this framework was then applied in the simplified ASOP multi-body seakeeping optimization study.

2 BACKGROUND

2.1 *AEGIR seakeeping code*

AEGIR, based on a three-dimensional non-uniform rational B-spline (NURBS) geometry engine, solves for wave-body interaction through a time-domain, potential-flow, Rankine boundary element approach. This is a geometry-independent method based on Maniar (1995) that applies the body-boundary conditions directly on the exact computer-aided design (CAD) surfaces. The high-order hydrodynamic boundary element method overlays the NURBS geometry

and yields stable wave and motion integration in time (Nakos 1990, Kring 1995). AEGIR also has a steady free-surface boundary condition that is used to predict steady wave resistance and wave patterns. The NURBS geometry engine in AEGIR automatically recomputes the waterline intersection and wetted body surface area at each time step, so a range of linear to fully nonlinear seakeeping formulations can be examined.

Although AEGIR's core solution is for potential-flow wave-body interactions, viscous forces, mooring lines, tethers, and other physical effects are incorporated within the seakeeping simulations through a combination of internal and external models. External models, such as control algorithms and dynamic models for various mechanical systems, may be coupled to AEGIR using the sockets interprocess communication library.

2.2 ASOP concept

We selected the ASOP concept, a novel, patented offshore platform concept (Grinius & Lynch 1995), as the basis for our multi-body seakeeping optimization study for two principal reasons: (1) it features the multiple, independently moving bodies that we wished to model, and (2) model test data was available to validate the enhanced AEGIR code. Figure 1 shows the four-float ASOP configuration that was tested in a seakeeping model basin. Note the key ASOP features: a submerged lower hull, supporting columns that in turn support an upper deck, and a set of articulated floats connected to the hull by means of flexible connectors that move freely and independently in the presence of waves. The full-scale design upon which the physical model was based displaces 45,087 t, with pontoon length of 99 m and diameter of 11.5 m and float length and diameter of 30.5 m and 17.2 m, respectively.

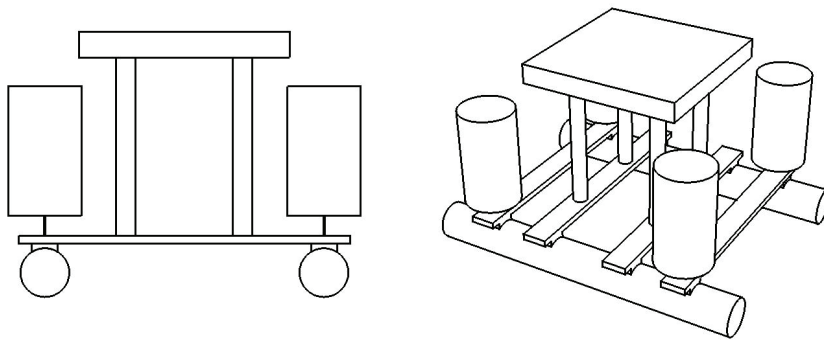


Figure 1. Four-float ASOP configuration

2.3 Hydrodynamic optimization

Improvements in potential-flow and viscous-flow models, improvements in microprocessor speed, and the availability of high-performance computing platforms, have made simulation-based hydrodynamic optimization of real ship applications feasible. Global search algorithms, combined with low- or medium-fidelity analysis models, can be used effectively in early design phases, whereas higher fidelity models would be desirable in later phases of the design.

Steady resistance is most commonly used as the objective function in hydrodynamic optimizations, although there are several examples of alternative single- and multi-objective functions in the literature. Minami & Hinatsu (2002) demonstrated multi-objective optimization of the Wigley and Series 60 hulls using steady resistance, added resistance, and ship motions. Steady resistance was computed using a three-dimensional Reynolds-Averaged Navier-Stokes code while seakeeping was predicted using a two-dimensional potential-flow strip theory. Seakeeping optimization of the S175 containership, using a three-dimensional frequency-domain panel code (Peri & Campana 2005) and two-dimensional strip theory (Pinto et al. 2007) to estimate heave and pitch response, was demonstrated. The authors have recently demonstrated optimization of multi-hulls using AEGIR to predict steady resistance for a range of speeds and seakeeping motions in sea state 4 as part of the High Speed Sea Lift project sponsored by the Office of Naval Research (Connell & Milewski 2008). In this instance, steady resistance and Motion Sickness Incidence were combined into a composite objective function.

While early optimization efforts used local techniques such as gradient-based or simplex methods, the recent trend is to employ global optimization methods based on heuristic search methods such as Genetic Algorithm (GA), PSO, or hybrid techniques combining GA or PSO with local search methods. Early such efforts in hydrodynamics primarily used GAs, but more recently the focus has shifted to PSO. The authors implemented a constrained PSO algorithm using the Message Passing Interface protocol as part of the multi-hull optimization project previously mentioned (Connell & Milewski 2008).

The authors have also used optimization techniques to improve hydrodynamic efficiency in steady-flow conditions for a series of innovative ship design problems—PSO was the optimization methodology of choice, in part, because it is well suited for use on multiple-node computer clusters, running multiple analyses in parallel as noted above. One such example sought to improve the overall efficiency of a bow lifting body ship by changing the location and section shape of the lifting body. Wave cancellation effects of the lifting body were included through a nonlinear representation of the free surface; the objective function included large penalties on cavitation and separation, effectively excluding all design points with either condition.

3 SEAKEEPING OPTIMIZATION FRAMEWORK

There are several key elements in an effective optimization framework. These include definition of design variables and objective functions, selection of a computer model to evaluate hydrodynamic performance, selection of the optimization scheme, automated procedures to modify the geometry, and an overarching control process to handle perturbation of the optimization variables, geometry manipulation, generation of hydrodynamic analysis code input files, calls to the hydrodynamic analysis code, calculation of the objective function, tabulation of the results of each optimization iteration, and process termination when an optimum is reached. Figure 2 shows a broad schematic of the control process implemented for this project, using AEGIR as the hydrodynamic analysis code, which is intended to represent the principal elements of the process and the general flow of data. In the following sections we'll describe in more detail selection of the optimization methodology, automated geometry manipulation, objective function formulation, and implementation of the control process.

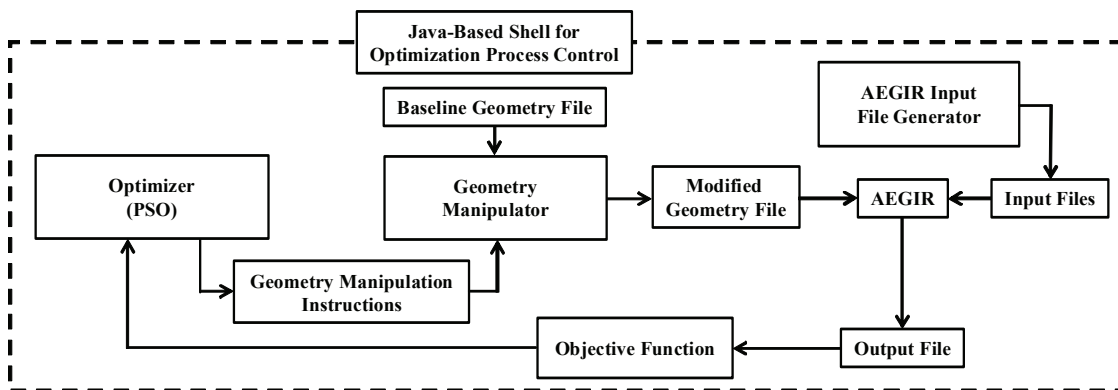


Figure 2. Optimization framework control process schematic

3.1 Particle swarm optimization

PSO is a simple, stochastic global optimization technique inspired by the flocking behavior of birds and fish (Kennedy & Eberhart 1995). The advantages of this methodology include: (1) the algorithm has constant computational cost and memory requirements at each iteration, (2) approximate solutions to the optimization problem are available after each iteration, (3) derivatives of the objective function are not required, and (4) it is easy to implement and parallelize (Pinto et al. 2007). The user defines a number of “particles” that are randomly distributed throughout the design space with random initial velocities. Each particle moves through the design space with some momentum, and attraction to two points in the design space: (1) the

local best, the location of the best objective function evaluation that the particle has experienced on its own track; and (2) the global best, the location of the best objective function evaluation that any of the particles have experienced. Each iteration of the PSO scheme represents a discrete time step of the particle motion through the design space, and as time progresses the particles swarm to the global maximum of the objective function. Weighting factors applied to the local best and global best terms in the particle equation of motion are multiplied by random numbers (hence the stochastic nature of the method).

PSO's inherent suitability for parallelization makes it attractive for application to complex engineering problems. It is generally accepted that twenty to forty particles are sufficient to realize almost any domain; a computer cluster running 40 cases in parallel can therefore complete an entire iteration in one pass. PSO also has the advantage of being extremely easy to implement, and a number of public-domain versions of the algorithm are freely available for download from the Internet. Finally, particle swarm optimization is relatively fast: for many engineering problems, PSO finds solutions reasonably close to the global maximum in just a few iterations. This last point, in particular, is what makes PSO such a compelling choice for application to complex engineering design problems—convergence on the mathematical global optimum is not necessary to obtain useful improvements if the objective function is properly constructed.

3.2 Geometry manipulation

Automated methods for creating hull or platform geometry and generating computational grids for the analysis code are integral components of the optimization process. Typically, hydrodynamic optimization begins with a baseline configuration, which is subsequently modified using information supplied by the optimization algorithm. An initial set of point designs is generated randomly throughout the design space at the beginning of the PSO algorithm, and new designs are created after each iteration.

The numerical grids for the body and free surface are generated directly in AEGIR, eliminating the need for external grid generation software. Automated grid generation is facilitated by two important features of the code: direct import of CAD files in Rhinoceros native file format, and integration of geometric algorithms in the code to handle trimmed NURB surfaces, e.g. point and derivative evaluations, intersections, etc. CAD geometry is modified outside AEGIR using a separate code based on the openNURBS library to modify the surfaces of the baseline configuration. Although we have a very general capability to manipulate B-spline surfaces, only procedures to stretch, rotate, and translate were used in this study.

3.3 Objective function formulation

One of the goals of this effort was to show that motions in a seaway (surge, sway, heave, roll, pitch, and yaw) can be reduced via a design optimization process. However, in some cases reducing velocities or accelerations could be as desirable as reducing motions. To accommodate such cases, we developed the general objective function given in Equation (1), where X is a weighting for modal displacement, V is a weighting for modal velocity, A is a weighting for modal acceleration, ξ_i is a vector of the root mean square (RMS) values of modal displacement, $\dot{\xi}_i$ is a vector of the RMS values of modal velocity, and $\ddot{\xi}_i$ is a vector of the RMS values of modal acceleration.

$$C = 100 - \left(\sum_{i=1..6} X_i \xi_i + \sum_{i=1..6} V_i \dot{\xi}_i + \sum_{i=1..6} A_i \ddot{\xi}_i \right) \quad (1)$$

Using this generalized equation, different weightings on position, velocity, and acceleration can be examined. For this study, only long-crested head seas were considered so sway (mode 2), roll (mode 4), and yaw (mode 6) could be ignored, leaving surge (mode 1), heave (mode 3), and pitch (mode 5). The choice of RMS values for use in the objective function was somewhat arbitrary, based on our experience with seakeeping performance; other approaches could have been selected that would have been equally valid.

3.4 Optimization control process

We implemented the optimization control process illustrated in Figure 2 using a custom, Java-based “shell” program to provide cross-platform compatibility since our computing resources include both Windows-based workstations and a Linux-based 64-node cluster. The user creates an optimization within the shell environment, specifying the baseline geometry file, the optimization design variables and their range, and the objective function. A custom geometry manipulation routine, as described in Section 3.2, is required for every new design problem. The shell program creates AEGIR input files for each particle, distributes the particles through the design space, and passes an entire iteration to the 64-node cluster; if the number of particles exceeds 64, the runs are submitted in batches. Each node executes an instance of AEGIR that performs a time-domain seakeeping simulation for the geometry represented by the specific point in the design space occupied by the particle at that iteration. Upon completion, AEGIR returns the time-series motions data to the shell program, which gathers results from all nodes (particles) and computes the objective function, Equation (1), for each particle. If the AEGIR simulation for an individual particle does not return a valid data set, due to a faulty node, ill-defined problem, or other error, that run is given a very poor objective function value. Because PSO allows for large discontinuities in the design space, this does not affect the overall solution. The shell program tracks the progress of the optimization, and terminates the process when specified convergence criteria are met.

4 SEAKEEPING OPTIMIZATION STUDY

4.1 Model problem formulation

For this study, we limited the number of design variables to two so the design space could be plotted easily and any trends readily visualized. However, limiting a geometry as complex as the one shown in Figure 1 to just two variables is almost impossible. Therefore, we selected a simplified problem using a two-float version of ASOP: a single submerged pontoon with a cylindrical float attached near each end. This configuration encompasses key aspects of the more complex multiple-float configuration—float separation, float radius, and float buoyancy as a percentage of total buoyancy—and captures what we think are the dominant variables in the system, pontoon length and float radius. Pontoon radius is a dependent variable and is adjusted to keep the overall system volume constant. A further simplification kept the center of gravity and radii of gyration of the bodies constant. Figure 3 shows a sketch of the two-float ASOP. This configuration demands the use of a nonlinear, time-domain seakeeping simulation because the linear hydrostatic and gravitational restoring of the tethered floats are negligible compared to the higher-order effects. Also, the close placement of the surface-piercing bodies requires a fully three-dimensional solution that allows for wave interaction. The enhanced AEGIR seakeeping simulation provides the necessary modeling fidelity.

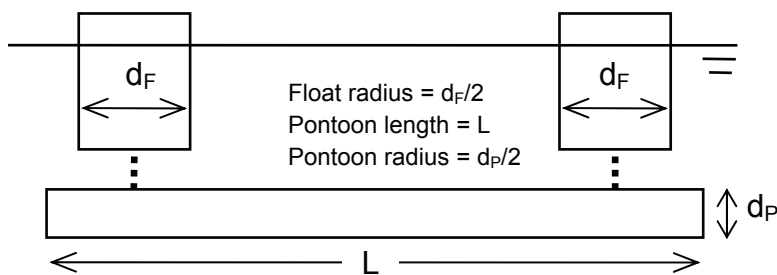


Figure 3. Simplified two-float ASOP configuration (not to scale)

Varying the float radius allows the percentage of total buoyancy supported by the floats to be changed. Because total volume is held constant, pontoon radius directly controls separation between the floats. A secondary effect of varying the float radius is a change in waterplane area. The range in variation of float radius and pontoon radius for the optimization study was from 80% to 120% of the baseline values.

4.2 Seakeeping response of baseline configuration

The baseline configuration was chosen so that the float radius and pontoon length were equal to the full-scale four-float configuration; values of 8.6 m and 99 m respectively. This constrained the displaced volume to be half that of the four-float configuration. For the incident wave system, we selected a Bretschneider spectrum with significant wave height and period chosen to be similar to those a real system would encounter (3.25 m and 9.7 sec, respectively). For the baseline case, the AEGIR simulation yielded RMS values for surge, heave, and pitch of 8.62 m, 8.12 m, and 18.7 deg, respectively.

4.3 Seakeeping response of optimized configurations

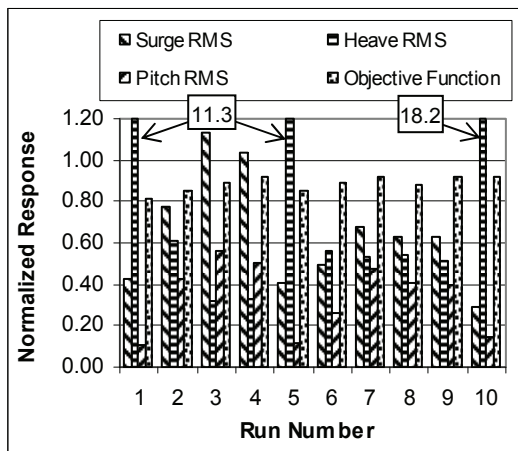
For this study, we constructed a set of objective functions using Equation (1) based solely on positions ($V_i \equiv 0, A_i \equiv 0$) and we limited our consideration to head seas as noted previously. We were interested in the effects of different objective function multipliers on the outcome of the optimization, so we systematically varied those multipliers—the set of multipliers that we selected was $X_{1,3,5} = \{0, \frac{1}{3}, \frac{2}{3}, 1\}$; these were constrained such that their sum was unity. This resulted in ten objective functions for a sequence of optimization runs with the multipliers as shown in Table 1. The optimizations were set up using 20 particles and a duration of 24 hours (approximately 48 iterations) for each run. We applied the same input wave spectrum as in Section 4.2 so that the results of the optimizations could be compared with the baseline.

The results from this series of optimizations are shown in Figure 4(a). For each optimization run, the individual RMS values for surge, heave, and pitch motions and the computed objective function value have been normalized by the corresponding values from the baseline case.

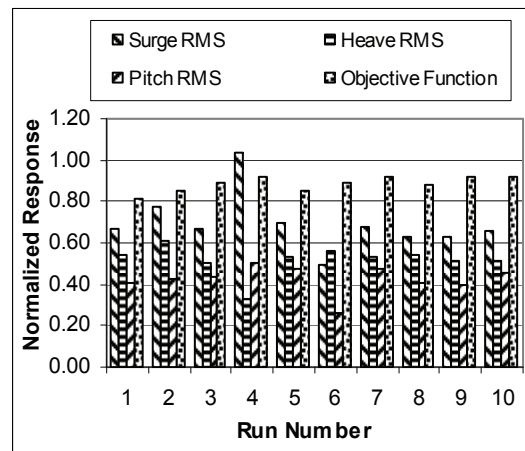
Looking at runs 1, 5, and 10, we see very large RMS heave motions relative to the baseline case—an order of magnitude higher. Upon closer inspection of these runs, we found that the assumption of small motions about the mean position had been violated. In these runs, the heave component multiplier is zero, eliminating any possible influence of heave on the objective function and thus allowing these invalid runs in the feasible solution set. To correct this issue, the matrix of objective function multipliers was adjusted as shown in Table 2.

Table 1. Optimization sequence—objective function multipliers

Run	X_1	X_3	X_5	Run	X_1	X_3	X_5	Run	X_1	X_3	X_5
1	0	0	1	5	0.33	0	0.67	8	0.67	0	0.33
2	0	0.33	0.67	6	0.33	0.33	0.33	9	0.67	0.33	0
3	0	0.67	0.33	7	0.33	0.67	0	10	1	0	0
4	0	1	0								



(a) Original optimization sequence



(b) Adjusted optimization sequence

Figure 4. Normalized response for all optimizations

Table 2. Optimization sequence—adjusted objective function multipliers

Run	X_1	X_3	X_5	Run	X_1	X_3	X_5	Run	X_1	X_3	X_5
1	0	0.10	0.90	5	0.28	0.10	0.62	8	0.67	0	0.33
2	0	0.33	0.67	6	0.33	0.33	0.33	9	0.67	0.33	0
3	0	0.67	0.33	7	0.33	0.67	0	10	0.90	0.10	0
4	0	1	0								

The results from this second series of optimizations are shown in Figure 4(b); we can see the excessively large RMS heave values have been eliminated. It is clear, in run 4, that surge is not being included in the objective function. Interestingly, in runs 1-3, when surge is also ignored, the surge motions are still reduced. In these runs, pitch is included, while it is not in run 4. This implies that by reducing pitch motions, surge motions are kept in check. In run 1, only pitch motions are controlled. However, in run 6, we see lower pitch motions than run 1. This indicates that our solver became stuck at a local maximum and never discovered the global maximum. The parameters to the PSO should be altered and the case should be rerun. In almost all cases, the components of the objective function for the optimized configurations are better than the baseline (only surge in run 4 has not been reduced), including when the multipliers in the objective function are zero. In general, multiple-component objective functions lead to clusters of valid optimizations, not a single point design. Because of this behavior, spotting trends in the solution space can be difficult.

Figure 5 shows the Pareto front for the general objective function as three planar views. Parameters plotted are un-weighted RMS surge, heave, and pitch values for the twenty best particles from each of the ten optimization runs. The front is not fully resolved, but the general shape is evident. In the heave/pitch plane, we see a vertical front line and a horizontal front line; we see a similar shape in the heave/surge plane. These lines indicate the series of designs that have similar worth, so depending on the designer's goal a number of different designs could be chosen. For example, from the heave/surge plot if the goal is to restrict surge then there is a trade-off allowing more heave. Similarly, from the heave/pitch plot if the goal is to restrict pitch then there is a trade-off allowing more heave. The wedge-shape of the Pareto front in the surge/pitch plane reflects the correlation between reduced surge and pitch motions discussed above. When performing multi-variable optimizations with multiple-component objective functions, a single optimum is never found. Rather, a series of good designs are identified, leaving it to the designer to make an appropriate choice.

It is also useful to examine the behavior of a single optimization run. Figure 6 shows a plot of the normalized values for surge, heave, and pitch motions for the best design at each iteration for optimization run 5. Also shown are the total normalized objective function value at each iteration and the normalized cumulative global best up to and including the current iteration. This plot shows that the best design is achieved at iteration 36; however, after iteration 23 the solution changes very little. Because of the long simulation run times, in practice the optimization is often not allowed to run to full convergence; however, if a design is found that is better than the original and is considered producible, the optimization is considered successful.

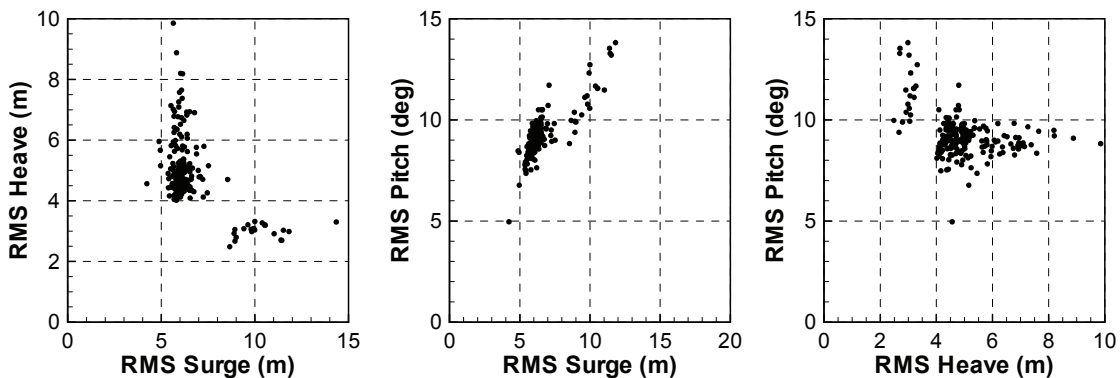


Figure 5. Pareto front plots: heave vs. surge, pitch vs. surge, pitch vs. heave

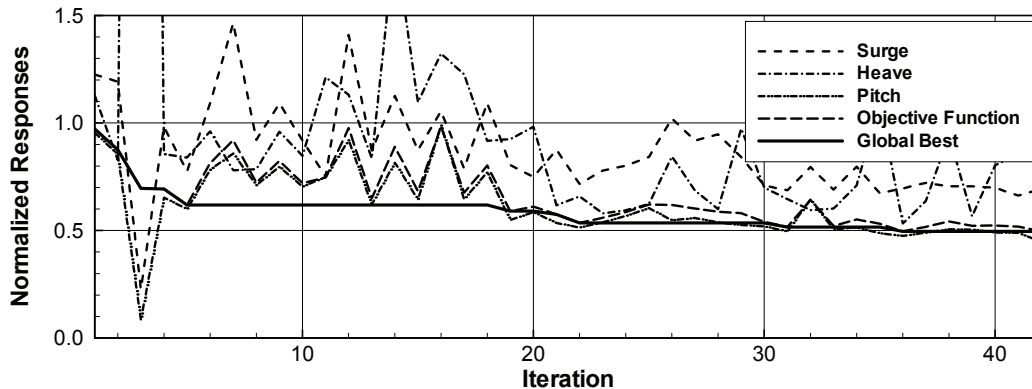


Figure 6. Best values by iteration for optimization run 5 (normalized to baseline)

5 CONCLUSIONS

Optimizing a simplified offshore platform for reduced motions has been achieved. Because of the presence of multiple bodies and the importance of free surface hydrodynamics a fully nonlinear, time-domain, free surface code was necessary. By looking at RMS motions, specific criteria can be met. By changing the objective function, very different designs can be found. For the purposes of this study, a systematic series of objective functions was tested, but the designer should tailor the objective function to meet specific design goals. This includes changing the criteria (in this case RMS motions) and changing the weighting on different aspects of the design. Trends in the individual optimizations and series of optimizations can be difficult to identify because the design space for these problems is often complex. As with any optimization, understanding the limitations of the tool used to compute the objective function is paramount. The user must be able to anticipate those limitations when formulating the objective function. Because of the long run times, it is not always possible to allow for a converged optimization. In practice, if the design is improved, the optimization is considered successful.

REFERENCES

- Connell, B. & W.M. Milewski. 2008. Multivariate design optimization with application to SWATH high speed sealift. Presentation to Office of Naval Research under Contract No. N00014-08-C-0086.
- Grinius, V. & A.C. Lynch. 1995. Semi-submersible offshore platform with articulated buoyancy. US Patent 5,435,262.
- Kennedy, J. & R. Eberhart. 1995. Particle swarm optimization. In *Proceedings, IEEE International Conference on Neural Networks (Perth, Australia): 1942-1948*. Piscataway, NJ: IEEE Service Center.
- Kring, D.C. 1995. Numerical stability analysis for time-domain ship motion simulations. *J. of Ship Research*, 39(4): 313-320.
- Maniar, H. 1995. A three dimensional higher order panel method based on B-splines. PhD thesis, Massachusetts Institute of Technology.
- Minami, Y. & M. Hinatsu. 2002. Multi objective optimization of ship hull form design by response surface methodology. In *24th Symposium on Naval Hydrodynamics: 977-990*. Washington, DC: The National Academies Press.
- Nakos, D.E. & P.D. Sclavounos. 1990. Ship motions by a three-dimensional Rankine panel method. In *18th Symposium on Naval Hydrodynamics: 21-40*. Washington, DC: The National Academies Press.
- Peri, D. & E.F. Campana. 2005. High-fidelity models and multiobjective global optimization algorithms in simulation-based design. *J. of Ship Research*, 49(3), pp. 159-175.
- Pinto, A., D. Peri & E.F. Campana. 2007. Multiobjective optimization of a containership using deterministic particle swarm optimization. *J. of Ship Research*, 51(3): 217-228.